

1
2
3
4
5
6
7
8
9
10
11
12
13
14
15
16
17
18
19
20
21
22
23
24
25

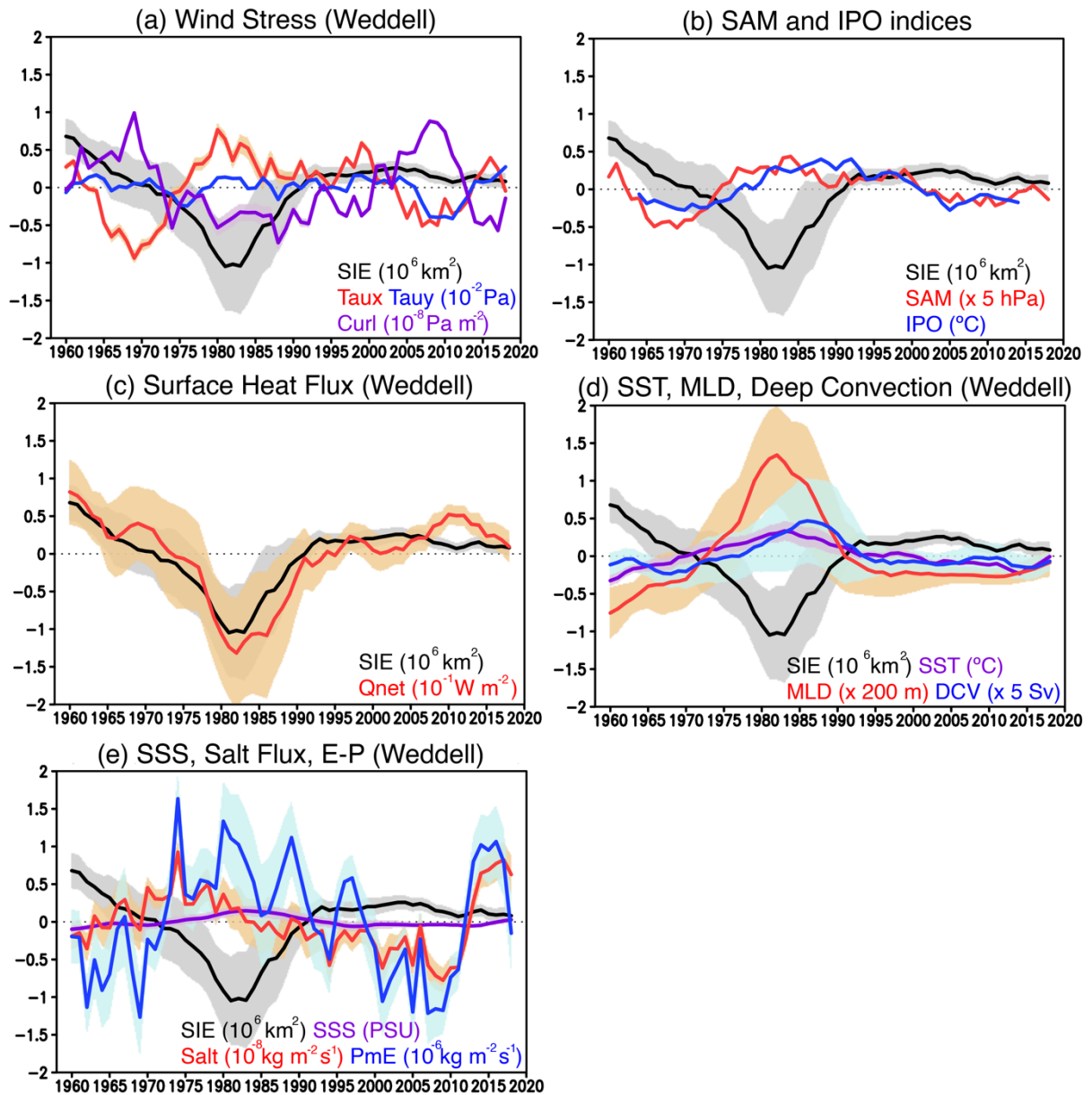
Supplement
for the reply to Reviewer 1's comments

Multidecadal Variability and Predictability
of Antarctic Sea Ice in GFDL SPEAR_LO Model

Yushi Morioka^{1,2,3}, Liping Zhang^{2,4}, Thomas L. Delworth²,
Xiaosong Yang², Fanrong Zeng², Masami Nonaka¹, Swadhin K. Behera¹

- 1: Application Laboratory, VAIg, JAMSTEC, Yokohama, Kanagawa, Japan
- 2: Geophysical Fluid Dynamics Laboratory, NOAA, Princeton, New Jersey, USA
- 3: Atmospheric and Oceanic Sciences Program, Princeton University,
Princeton, New Jersey, USA
- 4: University Corporation for Atmospheric Research, Boulder, Colorado, USA

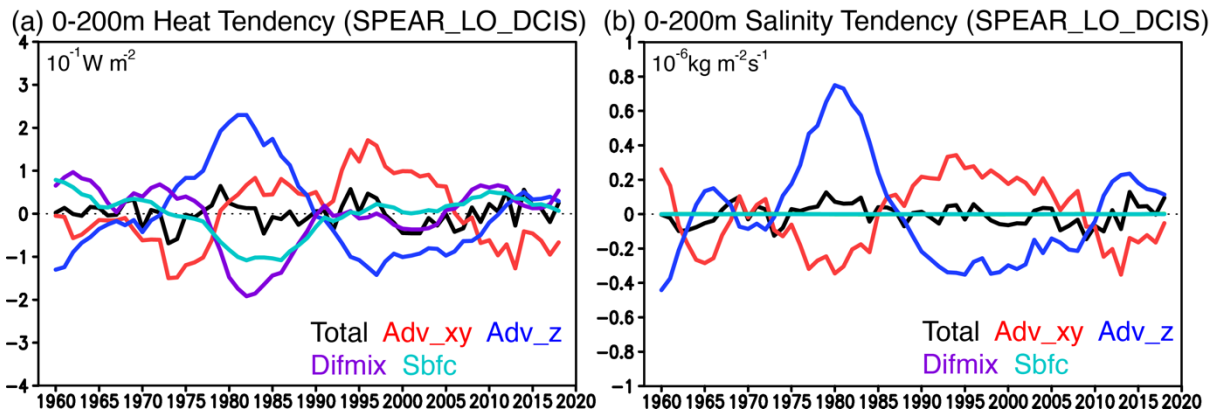
Apr 17, 2023
Submitted to The Cryosphere



26

27 **Figure 3 (a)** Time series of 5-yr running mean SIE (black in 10^6 km^2), zonal (Taux; red in 10^{-2}
 28 10^{-2} Pa) and meridional (Tauy; blue in 10^{-2} Pa) wind stress, and wind stress curl (Curl; purple in
 29 10^{-8} Pa m^2) anomalies averaged in the Weddell Sea ($60^\circ\text{W}-0^\circ$, south of 55°S) during 1958-
 30 2020. Shades indicate one and minus one standard deviations of the anomalies from 30
 31 ensemble members of the SPEAR_LO_DCIS. Positive wind stress curl anomalies correspond
 32 to downwelling anomalies in the ocean. **(b)** Same as in **(a)**, but for the 5-yr running mean SAM
 33 index (red in 5 hPa) and 13-yr running mean IPO index (blue in $^\circ\text{C}$). **(c)** Same as in **(a)**, but for
 34 the SIE (black in 10^6 km^2) and the net surface heat flux (Qnet; red in 10^{-1} W m^{-2}) anomalies.
 35 Positive surface heat flux anomalies correspond to more heat going into the ocean. **(d)** Same
 36 as in **(a)**, but for the SIE (black in 10^6 km^2), sea surface temperature (SST; purple in $^\circ\text{C}$), mixed-
 37 layer depth (MLD; red in 200 m), and deep convection (DCV; blue in 5 Sv) anomalies. **(e)**

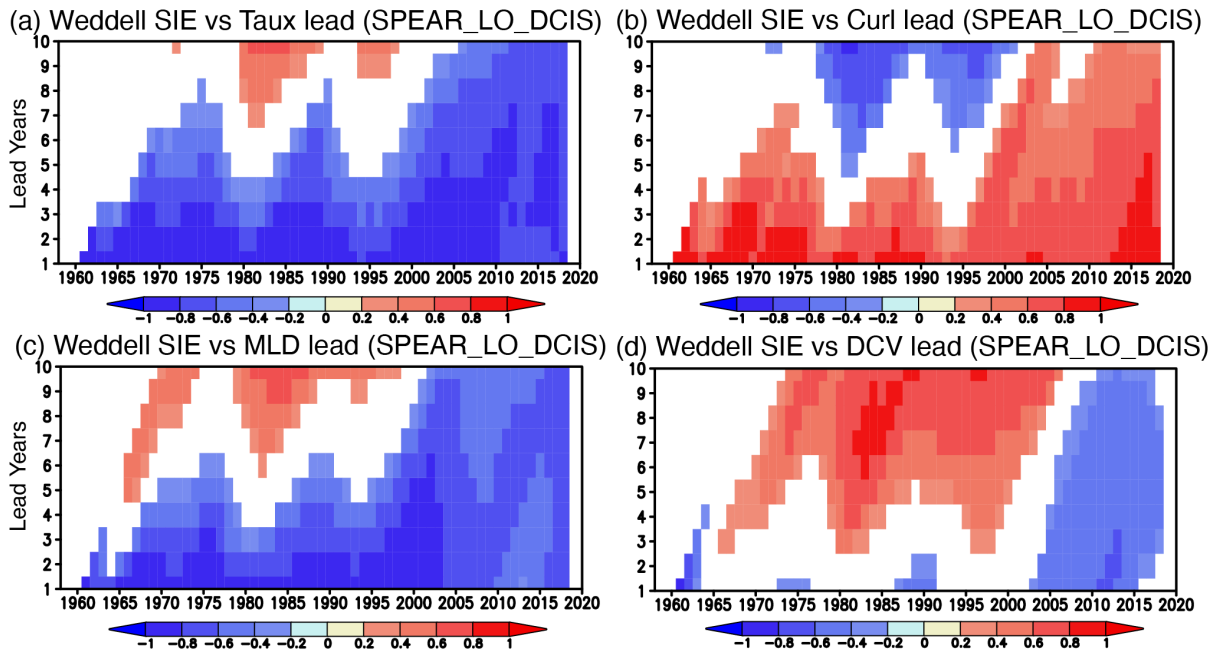
38 Same as in **(a)**, but for the SIE (black in 10^6 km²), sea surface salinity (SSS; purple in PSU),
39 salt flux (Salt; red in 10^{-8} kg m⁻² s⁻¹), and precipitation minus evaporation (PmE; blue in 10^{-6}
40 kg m⁻² s⁻¹) anomalies. Positive salt flux anomalies correspond to anomalous salt going into the
41 ocean at the surface associated with sea ice formation, whereas the positive PmE anomalies
42 mean more freshwater going into the ocean.
43



44

45 **Figure 6 (a)** Time series of 5-yr running mean ocean heat tendency (in 10^{-1} W m^{-2}) anomalies
 46 in the upper 200 m of the Weddell Sea from the SPEAR_LO_DCIS. Total ocean heat tendency
 47 (Total; black), horizontal advection (Adv_xy; red), vertical advection (Adv_z; blue), mesoscale
 48 diffusion and dianeutral mixing (Difmix; purple), and surface boundary forcing (Sbfc; light
 49 blue) anomalies are shown, respectively. **(b)** Same as in **(a)**, but for the salinity tendency (in
 50 $10^{-6} \text{ kg m}^{-2} \text{ s}^{-1}$) anomalies.

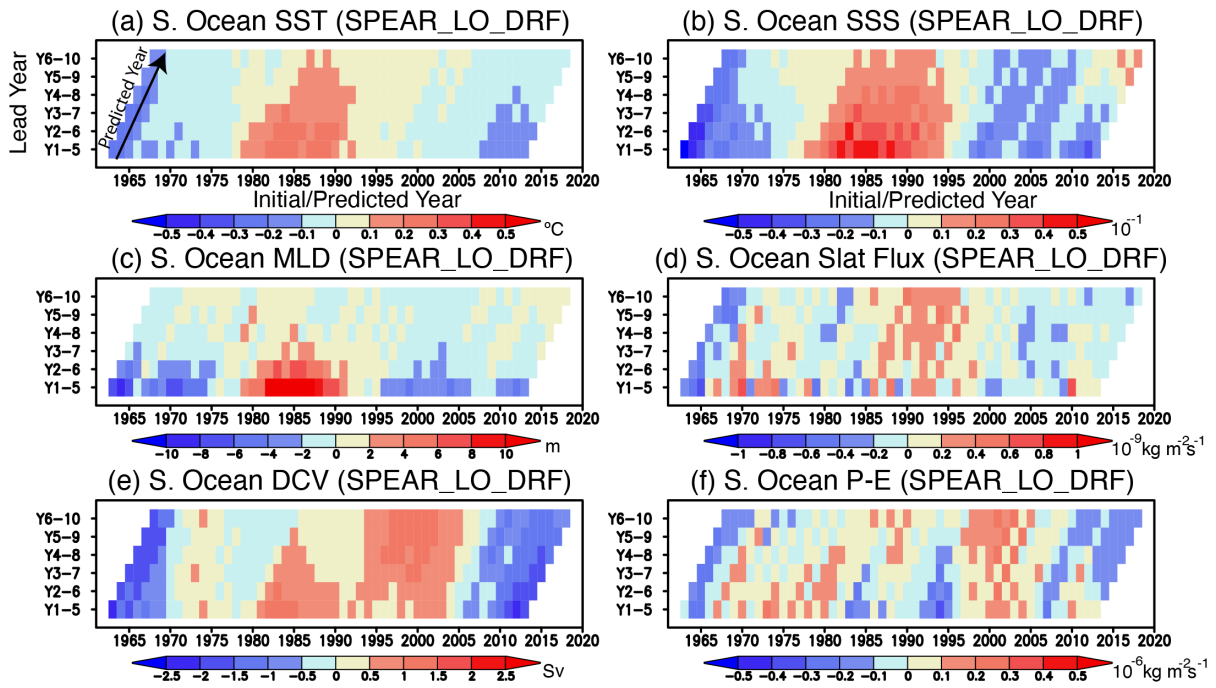
51



52

53 **Figure 7 (a)** Temporal evolution of inter-member correlation between the 5-yr running mean
 54 SIE anomalies and the 5-yr running mean zonal wind stress (Taux) averaged in the Weddell
 55 Sea from 30 ensemble members of the SPEAR_LO_DCIS as a function of lead years. Positive
 56 lead years (Y-axis) mean that the Taux anomalies lead the SIE anomalies by the number of
 57 years. Correlation coefficients that are statistically significant at 90 % using Student's *t*-test are
 58 shown in color. **(b)** Same as in **(a)**, but for the inter-member correlation between the SIE
 59 anomalies and the wind stress curl (Curl) anomalies. **(c)** Same as in **(a)**, but for the inter-
 60 member correlation between the SIE anomalies and the mixed-layer depth (MLD) anomalies.
 61 **(d)** Same as in **(a)**, but for the inter-member correlation between the SIE anomalies and the
 62 deep convection (DCV) anomalies.

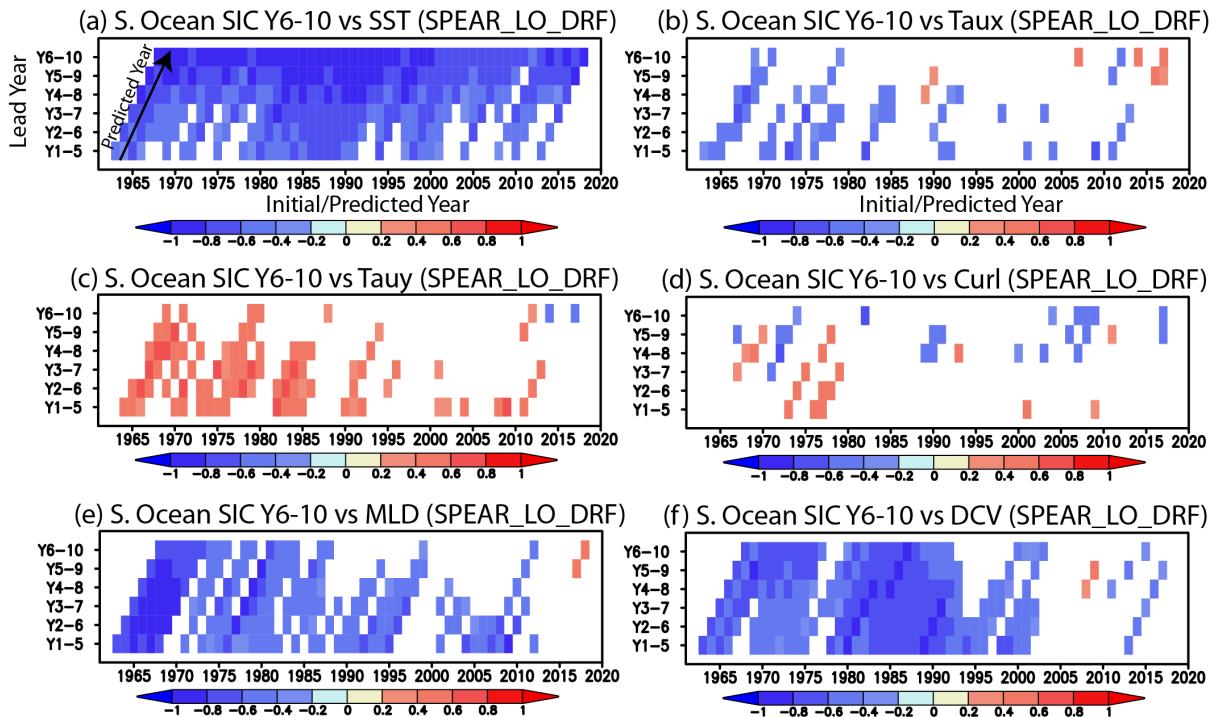
63



64

65 **Figure 11 (a)** Temporal evolution of ensemble mean Southern Ocean (south of 55°S) SST
 66 anomalies predicted at lead times from 1-5 years to 6-10 years in the SPEAR_LO_DRF as a
 67 function of initial/predicted years (x-axis) and lead years (y-axis). A black arrow indicates the
 68 correlations with the same initial year for different lead times, while the corresponding x-axis
 69 indicates the predicted years. **(b-f)** Same as in **(a)**, but for the SSS (in 10^{-1} PSU), mixed-layer
 70 depth (MLD; in m), salt flux (in 10^{-9} $\text{kg m}^{-2} \text{s}^{-1}$), deep convection (DCV; in Sv), and
 71 precipitation minus evaporation (P-E; in 10^{-6} $\text{kg m}^{-2} \text{s}^{-1}$) anomalies averaged in the Southern
 72 Ocean, respectively.

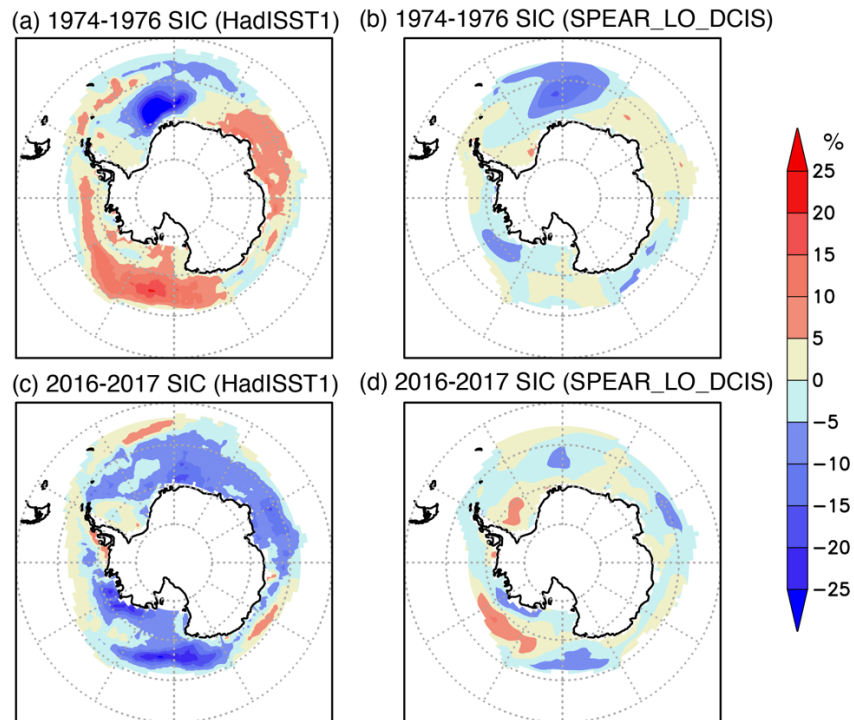
73



74

75 **Figure 12 (a)** Temporal evolution of inter-member correlation between the pan-Antarctic SIC
 76 anomalies predicted at a lead time of 6-10 years and the Southern Ocean SST anomalies
 77 predicted at lead times from 1-5 years to 6-10 years for the 20 ensemble members of the
 78 SPEAR_LO_DRF as a function of initial/predicted years (x-axis) and lead years (y-axis). A
 79 black arrow indicates the correlations with the same initial year for different lead times, while
 80 the corresponding x-axis indicates the predicted years. Correlation coefficients that are
 81 statistically significant at 90 % using Student's *t*-test are colored. **(b-f)** Same as in **(a)**, but for
 82 the inter-member correlation with the zonal wind stress, meridional wind stress, wind stress
 83 curl, mixed-layer depth, and deep convection anomalies averaged in the Southern Ocean.

84



85

86 **Figure S4 (a)** Sea ice concentration (SIC, in %) anomaly averaged over 1974-1976 from the
 87 HadISST1. **(b)** Same as in **(a)**, but for the SIC from the SPEAR_LO_DCIS. **(c, d)** Same as in
 88 **(a, b)**, but for the SIC anomalies averaged over 2016-2017.

89